

UC Irvine

UC Irvine Previously Published Works

Title

Peptide Derivatives of Retinylamine Prevent Retinal Degeneration with Minimal Side Effects on Vision in Mice.

Permalink

<https://escholarship.org/uc/item/9q3156xd>

Journal

Bioconjugate Chemistry, 32(3)

Authors

Yu, Guanping

Gao, Song-Qi

Dong, Zhiqian

et al.

Publication Date

2021-03-17

DOI

10.1021/acs.bioconjchem.1c00043

Peer reviewed



HHS Public Access

Author manuscript

Bioconj Chem. Author manuscript; available in PMC 2022 March 17.

Published in final edited form as:

Bioconj Chem. 2021 March 17; 32(3): 572–583. doi:10.1021/acs.bioconjchem.1c00043.

Peptide Derivatives of Retinylamine Prevent Retinal Degeneration with Minimal Side Effects on Vision in Mice

Guanping Yu,

Department of Biomedical Engineering, School of Engineering, Case Western Reserve University, Cleveland, Ohio 44106, United States

Song-Qi Gao,

Department of Biomedical Engineering School of Engineering, Case Western Reserve University, Cleveland, Ohio 44106, United States

Zhiqian Dong,

Center for Translation Vision Research, Gavin Herbert Eye Institute, Departments of Ophthalmology, Physiology & Biophysics, and Chemistry, University of California, Irvine, California 92697, United States

Li Sheng,

Department of Biomedical Engineering, School of Engineering, Case Western Reserve University, Cleveland, Ohio 44106, United States

Da Sun,

Department of Biomedical Engineering, School of Engineering, Case Western Reserve University, Cleveland, Ohio 44106, United States

Ning Zhang,

Department of Pharmacology, School of Medicine, Case Western Reserve University, Cleveland, Ohio 44106, United States

Jianye Zhang,

Center for Translation Vision Research, Gavin Herbert Eye Institute, Departments of Ophthalmology, Physiology & Biophysics, and Chemistry, University of California, Irvine, California 92697, United States

Seunghee Margeivicus,

Department of Epidemiology and Biostatistics, School of Medicine, Case Western Reserve University, Cleveland, Ohio 44106, United States

Corresponding Authors Krzysztof Palczewski – Center for Translation Vision Research, Gavin Herbert Eye Institute, Departments of Ophthalmology, Physiology & Biophysics, and Chemistry, University of California, Irvine, California 92697, United States; Phone: 949-824-6527; kpalczew@uci.edu; **Zheng-Rong Lu** – Department of Biomedical Engineering, School of Engineering, Case Western Reserve University, Cleveland, Ohio 44106, United States; Phone: (216) 368-0187; zx1125@case.edu.

Supporting Information

The Supporting Information is available free of charge at <https://pubs.acs.org/doi/10.1021/acs.bioconjchem.1c00043>.

Synthesis of Ret-NH₂ derivatives and emixustat-VG, HPLC and spectroscopic data and copies of ¹H and ¹³C NMR spectra and MS for all new compounds, LC-MS analysis of the Ret-NH₂ derivatives from the eye extraction, and **RVG** and Ret-NH₂ stability for storage (PDF)

The authors declare no competing financial interest.

Pingfu Fu,

Department of Epidemiology and Biostatistics, School of Medicine, Case Western Reserve University, Cleveland, Ohio 44106, United States

Marcin Golczak,

Department of Pharmacology, School of Medicine, Case Western Reserve University, Cleveland, Ohio 44106, United States

Akiko Maeda,

Center for Translation Vision Research, Gavin Herbert Eye Institute, Departments of Ophthalmology, Physiology & Biophysics, and Chemistry, University of California, Irvine, California 92697, United States; Department of Ophthalmology, School of Medicine, Case Western Reserve University, Cleveland, Ohio 44106, United States

Krzysztof Palczewski,

Center for Translation Vision Research, Gavin Herbert Eye Institute, Departments of Ophthalmology, Physiology & Biophysics, and Chemistry, University of California, Irvine, California 92697, United States

Zheng-Rong Lu

Department of Biomedical Engineering, School of Engineering, Case Western Reserve University, Cleveland, Ohio 44106, United States

Abstract

Safe and effective molecular therapeutics for prophylactic treatment of retinal degenerative diseases are greatly needed. Disruptions in the clearance of all-*trans*-retinal (atRAL) by the visual (retinoid) cycle of the retina can lead to the accumulation of atRAL and its condensation products known to initiate progressive retinal dystrophy. Retinylamine (Ret-NH₂) and its analogues are known to be effective in lowering the concentration of atRAL within the eye and thus preventing retinal degeneration in mouse models of human retinopathies. Here, we chemically modified Ret-NH₂ with amino acids and peptides to improve the stability and ocular bioavailability of the resulting derivatives and to minimize their side effects. Fourteen Ret-NH₂ derivatives were synthesized and tested *in vitro* and *in vivo*. These derivatives exhibited structure-dependent therapeutic efficacy in preventing light-induced retinal degeneration in *Abca4*^{-/-}*Rdh8*^{-/-} double-knockout mice, with the compounds containing glycine and/or *L*-valine generally exhibiting greater protective effects than Ret-NH₂ or other tested amino acid derivatives of Ret-NH₂. Ret-NH₂-*L*-valylglycine amide (**RVG**) exhibited good stability in storage; and effective uptake and prolonged retention in mouse eyes. **RVG** readily formed a Schiff base with atRAL and did not inhibit RPE65 enzymatic activity. Administered by oral gavage, this retinoid also provided effective protection against light-induced retinal degeneration in *Abca4*^{-/-}*Rdh8*^{-/-} mice. Notably, the treatment with **RVG** had minimal effects on the regeneration of 11-*cis*-retinal and recovery of retinal function. **RVG** holds promise as a lead therapy for effective and safe treatment of human retinal degenerative diseases.

Graphical Abstract

expressed in cell membranes and intestinal brush borders. These transporters have been targeted in designing ocular therapeutics with improved bioavailability.²¹ For example, modifications with valine significantly enhance oral bioavailability (F_o). Thus, conversion of acyclovir to valacyclovir²²⁻²⁴ increases F_o from ~16% to 54%, and for ganciclovir to valganciclovir from 6% to 61%.^{25,26} Also, modification of desglymidodrine with glycine to midodrine increased the oral bioavailability from 50% to 93%.²⁷ By analogy, structural modifications of Ret-NH₂ with amino acids or peptides that utilize the amino acid or peptide transporters could facilitate gastrointestinal absorption of these Ret-NH₂ derivatives and their uptake by the eye.^{19,28} Formation of an amide bond with the primary amine of Ret-NH₂ could improve its stability, especially in the gastric acidic environment after oral administration. Most importantly, this structural modification is expected to alleviate the inhibition of RPE65 in the visual cycle by blocking drug binding to the enzyme, thereby minimizing side effects.

Here, we designed and synthesized a library of 14 amino acid and peptide derivatives of Ret-NH₂ and then tested their efficacy in preventing light-induced retinal degeneration in *Abca4*^{-/-}*Rdh8*^{-/-} mice. Cell transport, uptake, and biodistribution of the lead derivatives were evaluated *in vitro* and *in vivo* in wild-type mice. The most promising candidate compounds were assessed *in vitro* and *in vivo* for sequestration of atRAL by Schiff base formation and for their potential effects on RPE65 and the visual cycle. Potential side effects on vision of the selected lead compounds were assessed also in wild-type mice. We also synthesized the L-Val-Gly peptide derivative of emixustat, an analogue of Ret-NH₂ and inhibitor of RPE65, and investigated its efficacy in preventing retinal degeneration in *Abca4*^{-/-}*Rdh8*^{-/-} mice.

RESULTS

Synthesis of Ret-NH₂ Derivatives and Emixustat-L-Val-Gly.

Fourteen amino acid and peptide derivatives of Ret-NH₂ (designated **3a–3n**) were synthesized by conjugating selected amino acids or peptides, as shown in Figure 1. Emixustat-L-Val-Gly amide was synthesized via the same method. Structures of the resulting derivatives are shown in Table 1. The synthesis involved reacting Ret-NH₂ or emixustat with *N*-fluorenylmethoxycarbonyl (Fmoc)-protected amino acids or peptides in the presence of coupling agents. The Fmoc group then was removed with 20% piperidine in ethyl acetate solution to provide the targeted molecules. The Ret-NH₂ derivatives and emixustat-L-Val-Gly were characterized by ¹H NMR, ¹³C NMR, and mass spectrometry (see the Supporting Information). The synthesized derivatives had a purity >95% as determined by HPLC, except for **3n**, Ret-Gly-Gly (**RGG**), whose purity was 90% (see the Supporting Information). Less than 5% degradation of **RVG** was observed when this compound was stored in a desiccator under vacuum at room temperature for 2 months, whereas 95% of Ret-NH₂ decomposed under the same conditions within 1 week (Figure S1).

Effects of Ret-NH₂ Analogues on Light-Induced Retinal Degeneration.

The effectiveness of Ret-NH₂ derivatives in preventing light-induced retinal degeneration was tested in four-week old *Abca4*^{-/-}*Rdh8*^{-/-} mice according to the experimental scheme

depicted in Figure 2a. After the mice were dark-adapted for 48 h, drugs were gavaged orally at a dose of 0.875 $\mu\text{mol}/\text{per mouse}$, which was selected based on the half-protective dose for Ret-NH₂ in a dose–response experiment (Figure 2b). Ret-NH₂ at the same molar dose was tested as a positive control for each derivative. Sixteen hours later, mice were exposed to light at 10 000 lx for 1 h and then kept in the dark for 3 days. Retinal integrity was then assessed using optical coherence tomography (OCT). Representative OCT images for **RVG** and both positive and negative illumination controls are shown in Figure 2c. The mice without light illumination possessed intact retinas and were used as positive controls. Mice without any treatment were used as negative controls and exhibited virtually complete destruction of photoreceptor cells after light illumination. Retinal integrity was determined based on the thickness of the outer nuclear layer (ONL) of the retinas measured from the OCT images; a reduced ONL thickness signifies a decreased number of photoreceptors and retinal degeneration. The white reflective layer in the retinas of negative control mice, which is thicker than a healthy outer plexiform layer (OPL), corresponds to the dying photoreceptor cells in the ONL. Ret-NH₂ derivatives showed a structure-dependent therapeutic protection against light-induced retinal degeneration (Figure 2d). The glycylyl, glycylylvalyl, and valylglycyl derivatives showed significantly better protection than either Ret-NH₂ or other derivatives of Ret-NH₂, with no visible damage at 4 locations around the optic nerve. In comparison, the phenylalanyl, D-alanyl, D-valyl, β -alanyl, and pregabalin derivatives had little protective efficacy. The protective efficacy for Ret-NH₂ amino acid or peptide conjugates from low to high are Ret-L-Phe, Ret-D-Ala, Ret-D-Val, Ret- β -Ala, Ret-Preg < Ret-L-Leu, Ret-L-Ile < Ret-L-Ala, Ret-L-Pro < Ret-NH₂ < Ret-L-Val < Ret-Gly-Gly < Ret-L-Val-Gly, Ret-Gly < Ret-Gly-L-Val.

The derivative **RVG** was selected as a lead agent for further detailed assessment because it is a solid at room temperature, whereas **RG** and **RGV** are both oils. Solid materials are generally preferred because of easy handling in drug development and clinical use. *Abca4*^{-/-}*Rdh8*^{-/-} mice were treated with **RVG** or Ret-NH₂. Sixteen hours later, mice were exposed to light at 10 000 lx for 1 h and then kept in the dark for 7 days. Retinal function was then assessed using electroretinograms (ERGs). Figure 3a shows average peak amplitudes of ERG scotopic a-waves for the mice in different treatment groups. ERG responses of mice treated with **RVG** and light illumination (LI) were virtually the same as in mice with no light-illumination (NLI), indicating that **RVG** did not inhibit the RPE65 activities. In contrast, the average ERG peak amplitudes were significantly lower for mice that were untreated or treated with Ret-NH₂ and then illuminated with strong light. Histological analyses also showed that mice treated with **RVG** maintained an intact retinal structure after exposure to intense light, while the retinas of mice without drug treatment had a markedly reduced ONL thickness after such light exposure (Figure 3b). These results demonstrate that Ret-NH₂ derivatives of glycine and/or valine, especially **RVG** at a reduced dose, showed remarkable efficacy in preventing light-induced retinopathy without inhibiting RPE65.

Biodistribution of RVG in Normal C57BL/6J Mice.

RVG and other selected Ret-NH₂ derivatives, either with a relatively high protective effect (**RG** and **RV**) or low protective effect (**RF** and **RL**) were administered via oral gavage to 4-

week-old C57BL/6J mice; then their biodistribution in the liver and eye was determined. Figure 4 shows the concentrations of the respective *N*-retinylamides, corresponding to the primary metabolites of Ret-NH₂^{14,29} and of each of its various synthetic derivatives, in the liver and eye at different time points (2 and 16 h) after gavage of the parent compounds. After 2 h, mice that received Ret-NH₂ had much higher liver concentrations of the corresponding *N*-retinylamides than did those that received the Ret-NH₂ derivatives, suggesting a more rapid absorption and/or metabolism of Ret-NH₂ after oral administration. The concentrations of *N*-retinylamides were increased in the liver of all treated mice at 16 h post-treatment. No *N*-retinylamides were detected in the eyes of any of the treated mice at 2 h. Interestingly, the derivatives **RVG**, **RG**, and **RV** with high protective effects on the retina displayed lower liver accumulations of *N*-retinylamides than did **RF** and **RL**, and **RVG** and **RV** produced no detectable *N*-retinylamides in the eye at 16 h. The lipophilic side chains of the amino acids in **RF** and **RL** might facilitate rapid metabolism of the conjugate and release of free Ret-NH₂ in the liver, with concomitant formation of *N*-retinylamides. In contrast, the derivatives **RF**, **RL**, and **RG** produced concentrations of *N*-retinylamides in the eye comparable to that of Ret-NH₂ at 16 h. Concentrations of the original drugs were also determined in the liver (c) and eye (d) at 2 and 16 h (Figure 4c,d). All tested drugs, including Ret-NH₂, were detected in the liver, and their concentrations decreased from 2 to 16 h. **RG** and **RV** were detected in the eyes at 2 and 16 h at relatively high concentrations. **RVG** was detected only at 16 h, whereas **RF** and **RL** were detected only at 2 h. No Ret-NH₂ was detected at 2 and 16 h in the eye, possibly because of rapid metabolism. The results indicate that Ret-NH₂ and the tested derivatives are readily absorbed into the body after oral gavage. The derivatives **RVG**, **RG**, and **RV** with good retinal protective effects show prolonged presence in the eye, while **RF** and **RL** with poor protective effectiveness are quickly metabolized in the liver into *N*-retinylamides, which was then transported in the eye. All tested drugs, including Ret-NH₂, were not detected in blood at 2 and 16 h.

***In Vitro* Caco-2 Cell Transport and ARPE-19 Cell Uptake.**

Transport and cellular uptake of **RVG**, **RF**, and Ret-NH₂ were investigated with Caco-2 cells, a human epithelial colorectal adenocarcinoma cell monolayer used as an *in vitro* model for oral gastrointestinal transport,^{27,30} and with ARPE19 cells, a modified human RPE cell line. As shown in Figure 5, both **RVG** and **RF** exhibited significantly higher transport through the Caco-2 monolayer and a higher uptake by ARPE19 cells than Ret-NH₂. There were no significant differences between **RVG** and **RF** in both cases. This result is consistent with the interpretation that the uptake of both derivatives of Ret-NH₂ was facilitated by peptide transporters.

Effects on the Retinoid Cycle.

The effect of **RVG** on the regeneration of 11-*cis*-retinol in the retinoid cycle was investigated *in vitro* by incubating this drug with RPE microsomes; Ret-NH₂ was used as control. The activity of RPE65-dependent isomerization of all-*trans*-retinol in the presence of retinaldehyde-binding protein^{31,32} was determined by monitoring 11-*cis*-retinol production by HPLC. Figure 6a shows percent of RPE65 activity (11-*cis*-retinol production) as a function of increasing concentrations of **RVG** or Ret-NH₂. As expected, addition of

Ret-NH₂ resulted in a concentration-dependent inhibition of RPE65, whereas **RVG** up to 10 μ M did not affect significant inhibition. Analogous results for Ret-NH₂ and **RVG** were obtained with NIH3T3 cells³² that stably express LRAT and RPE65. HPLC analysis of 11-*cis*-retinol production was easily detected in nontreated cells (control) and the cells treated with **RVG**, whereas the addition of Ret-NH₂ virtually ablated 11-*cis*-retinol production by inhibiting isomerase activity (Figure 6b). The inhibitory effect on RPE65 was further investigated in dark-adapted C57BL/6J wild-type mice after oral gavage of Ret-NH₂ and **RVG**. Figure 6c shows that mice treated with Ret-NH₂ produced a much lower concentration of 11-*cis*-retinal than the untreated controls, indicating a slow regeneration of 11-*cis*-retinal and a strong inhibitory effect of this drug on the retinoid cycle.³³ **RVG** allowed a greater regeneration of 11-*cis*-retinal in the eye, indicating less inhibition of the retinoid cycle than exhibited by Ret-NH₂ (Figure 6d).

In Vitro Schiff Base Formation with atRAL.

The above experiments revealed that **RVG** reduced 11-*cis*-retinal concentration in the eye but did not inhibit the activity of RPE65. We hypothesized that Ret-NH₂ and its amino acid (except proline) and peptide derivatives could also act as scavengers to sequester atRAL by forming Schiff base conjugates,¹⁰ thereby slowing down the retinoid cycle and reducing the atRAL concentration below the toxic level. Therefore, we assessed the ability of **RVG** and **RF** to form Schiff base adducts with atRAL. Figure 7 shows the HPLC chromatograms and UV-vis and mass spectra for reaction mixture of Ret-NH₂, **RF**, or **RVG** with atRAL. Schiff base adducts with atRAL were identified for all of the tested compounds (Ret-NH₂, **RVG**, and **RF**). The results indicate that the amino acid (except proline) and peptide conjugates of Ret-NH₂ could act as atRAL scavengers by forming Schiff base adducts.

Effects of Emixustat-L-Val-Gly Derivative.

Emixustat is an analogue of Ret-NH₂ and a modulator of the retinoid cycle. The *L*-Val-Gly derivative of emixustat (EVG) was synthesized and administered to *Abca4*^{-/-}*Rdh8*^{-/-} mice to assess how this chemical modification altered the drug's effects. Figure 8 shows that EVG exhibited protective efficacy against light-induced retinal degeneration relatively lower than that of emixustat at the same dose (1.9 μ mol/mouse). Although emixustat resulted in complete protection of the retinas from light-induced degeneration, the treatment greatly decreased the ERG activities, measured 7 days after the drug administration and illumination. In comparison, the treatment with EVG resulted in only slight decrease of ERG activities as compared with the untreated mice. The modification of emixustat with *L*-Val-Gly dipeptide might inhibit its binding to RPE65 and consequently diminish the morphological protective effect against retinal degeneration. Nevertheless, inhibition of strong binding of the EVG to RPE65 significantly reduced the side effects of the drug on vision.

DISCUSSION

Modulation of the retinoid cycle has been considered an effective approach for preventive treatment of retinal degeneration. Ret-NH₂ and its analogue emixustat (formerly ACU4429) have been identified as potent modulators of the retinoid cycle.^{11,34} Both compounds act as

inhibitors of RPE65 and can prevent retinal degeneration in experimental animals and human patients. However, a potential side effect of RPE65 inhibition is impairment of the retinoid cycle and consequent loss of night vision. We previously reported that atRAL, a potentially toxic but essential component of the retinoid cycle, can be sequestered by forming Schiff base adducts with primary amines such as Ret-NH₂, thereby effecting protection against retinal degeneration in animal models of AMD and Stargardt disease^{34,35}. This mechanism of action could minimize the potential side effects of RPE65 inhibition. Here, we chemically modified Ret-NH₂ with amino acids or peptides to improve its stability; therapeutic efficacy; and, most importantly, safety profile. We selected β -alanine, pregabalin, glycine, seven *L*-amino acids, two *D*-amino acids, and three dipeptides for these modifications and synthesized 14 Ret-NH₂ derivatives with different structures and configurations. The goal was to identify a stable derivative with high therapeutic efficacy and minimal side effects as a lead compound for preventing retinal degeneration.

We have found that these new Ret-NH₂ derivatives have several unique features compared to Ret-NH₂. The chemical stability of the amino acid and peptide derivatives is significantly improved over that of Ret-NH₂. Ret-NH₂ is readily protonated in aqueous solution under neutral or acidic conditions to form the ammonium cation, which can destabilize the conjugate polyene. Formation of an amide bond at the primary amine of Ret-NH₂ prevents protonation near the polyene and improves stability. The derivatives are readily absorbed by the body after oral administration, as observed with the tested compounds (Figure 4), a finding further validated with Caco-2 and ARPE-19 cells *in vitro* (Figure 5). The amino acid and dipeptide derivatives also have primary amine moieties that readily form Schiff base adducts to sequester atRAL, as demonstrated with **RVG** and **RF** (Figure 7). The chemical modifications of Ret-NH₂ also introduce steric hindrance for binding of the derivatives to RPE65, thereby diminishing the inhibitory effect associated with unsubstituted Ret-NH₂ and alleviating the risk for night blindness. The Phe derivative **RF** showed minor inhibitory effects on RPE65 isomerase activity *in vitro*, while the dipeptide derivative **RVG** possessed no inhibitory effect (Figure 6). The larger dipeptide derivatives have a greater steric effect than the amino acid derivatives on binding to RPE65; consequently, they produce little inhibition of this enzyme. **RVG** can sequester atRAL by forming a Schiff base adduct, while it displays little inhibition of RPE65. Thus, this conjugate seems to be a promising candidate to treat retinal degeneration with minimal side effects.

The Ret-NH₂ derivatives displayed structure-dependent relative efficacies for preventing light-induced retinal degeneration in *Abca4*^{-/-}*Rdh8*^{-/-} mice. **RVG**, **RG**, and **RGV** were significantly more effective than Ret-NH₂ at the same low dose in preventing retinal degeneration ($p < 0.05$). No visible damage was observed at four locations around the optic nerve in the retinas of mice treated with these compounds. Derivatives composed of amino acids other than glycine or *L*-valine were less protective than Ret-NH₂ itself. *D*-Valine derivatives had no protective efficacy as compared to their *L*-counterparts.

Our results are consistent with those reported by another research group who investigated amino acid- and peptide-containing ocular therapeutics in a different context³⁶. The protective effects we observed were positively correlated with the biodistribution of our derivatives to the eye, as shown in Figure 4. Strong light exposure for efficacy assessment

was performed at 16 h after oral gavage of the administered compounds (Figure 2a). **RG**, **RV**, and **RVG** were detected in the eye at that time, while **RF** and **RL** were not. The presence of the therapeutics in the eye at the time of exposure supports the interpretation that they could prevent retinal degeneration by sequestration of atRAL via Schiff base adduction. **RF** and **RL** were detected in mouse eyes at 2 h after gavage, whereas significant amounts of their *N*-retinylamide metabolites were found at 16 h. Both amino acids in **RF** and **RL** have lipophilic side chains, which might facilitate metabolic release of Ret-NH₂,³⁷ followed by the rapid conversion to *N*-retinylamides in the liver and eye. Therefore, although **RF** and **RL** were both initially present in eye, their rapid metabolism resulted in the conversion to *N*-retinylamides that lacked protective effects. Accordingly, **RF** and **RL** showed little protective effect under the experimental conditions we used. It appears that instead, **RV** and **RVG** are less lipophilic and resisted metabolic conversion in the eye such that no ocular *N*-retinylamides were detectable at both 2 and 16 h after oral gavage. Taken together, Ret-NH₂ derivatives with a prolonged presence in the eye after oral gavage were generally more effective in protecting the retina from light-induced degeneration.

Oral treatment with **RVG** resulted in slow regeneration of 11-*cis*-retinal *in vivo*. The inhibition by **RVG** could be attributed to sequestration of atRAL as the Schiff base adduct, accounting for the low concentration of atRAL; then slow hydrolysis of the Schiff base to release atRAL for isomerization would result in a slow regeneration of 11-*cis*-retinal. Nevertheless, the regeneration was significantly more rapid than that found with Ret-NH₂, allowing more rapid recovery of normal retinoid cycle function and mitigating potential side effects, including night blindness. Indeed, ERG tests demonstrated a rapid recovery of retinal function after the **RVG** treatment. These experiments provide evidence that the amino acid or peptide derivatives of Ret-NH₂, especially **RVG**, are effective in modulating the retinoid cycle and preventing retinal degeneration, with less likelihood of serious side effects.

The Ret-NH₂ analogue, emixustat, is currently under clinical trials for treating retinal degeneration in patients. Emixustat is a potent modulator of retinoid cycle and binds tightly to RPE65.³⁸ However, such strong binding of the drug to RPE65 may compromise the vision of patients.^{11,16} Chemical modification of the drug with L-Val-Gly decreases the preventative efficacy of the drug, possibly because of inhibition of the drug binding to RPE65. The modified drug EVG still maintains significant efficacy in preventing light-induced degeneration in *Abca4*^{-/-}*Rdh8*^{-/-} mice, likely through the mechanism of Schiff base formation with atRAL, which slows down the retinoid cycle. Consequently, treatment with EVG results in only a small decrease of ERG activity as compared to the control without light illumination. Thus, modification of emixustat with the dipeptide may alleviate the adverse effect of the drug on vision while providing significant therapeutic efficacy, potentially making EVG a safer alternative to emixustat in treating retinal degeneration in patients.

In summary, we synthesized and tested several amino acid and dipeptide derivatives of Ret-NH₂. The modified Ret-NH₂ derivatives possessed improved chemical stability. The derivatives with primary amines have the ability to sequester potentially toxic atRAL by Schiff base adduction. The derivatives showed structure-dependent efficacy in preventing

light-induced retinal degeneration in *Abca4^{-/-}Rdh8^{-/-}* mice. The glycy- and/or *L*-valyl-containing Ret-NH₂ derivatives displayed therapeutic efficacy higher than that of Ret-NH₂ and the other amino acid derivatives. This higher efficacy was correlated with relatively low metabolism of these derivatives within the eye. The derivative **RVG**, with a combination of superior pharmaceutical and pharmacological properties, is identified as a lead compound for further therapeutic development. **RVG** provided effective protection against retinal degeneration without inhibiting the RPE65 enzyme and caused minimal interference with retinoid cycle chemistry. Mice treated with **RVG** displayed a rapid regeneration of 11-*cis*-retinal and recovery of retinal function. Modification of emixustat with the valylglycyl dipeptide (**EVG**) diminished the side effects of the drug on vision. **RVG** and **EVG** could be promising therapeutics for prophylactic prevention of human retinopathy.

METHODS

Animals and Oral Administration.

Abca4^{-/-}Rdh8^{-/-} double knockout mice and C57BL/6J mice (female and male, 4 weeks old) (Jackson Laboratories, Bar Harbor, ME) were housed in the animal facility at the School of Medicine, Case Western Reserve University, where they were maintained either under complete darkness or on a 12 h light (~10 lx) and 12 h dark cycle. All animal procedures and experiments were approved by the Case Western Reserve University Animal Care Committees and conformed to recommendations of the American Veterinary Medical Association Panel on Euthanasia and the Association of Research for Vision and Ophthalmology. All tested compounds were dissolved or suspended in 100 μ L of vegetable oil with less than 10% (v/v) DMSO and were administered by oral gavage with a 22-gauge feeding needle. Experimental manipulations in the dark were done under dim red light transmitted through a Kodak No. 1 safelight filter (transmittance > 560 nm).

Induction of Light-Induced Retinal Degeneration in *Abca4^{-/-}Rdh8^{-/-}* Mice.

Female and male *Abca4^{-/-}Rdh8^{-/-}* mice (4 weeks old) were randomly assigned into different treatment groups. After dark adaptation for 48 h, *Abca4^{-/-}Rdh8^{-/-}* mice with pupils dilated by 1% tropicamide were exposed to fluorescent light (10 000 lx) for 60 min in a white plastic bucket with food and water and then kept in the dark. Histological and biochemical experiments were performed 3 days after light exposure.

Ultrahigh-Resolution Spectral-Domain OCT.

Ultrahigh-resolution spectral-domain OCT (SD-OCT; Bioptigen) was used for *in vivo* imaging of mouse retinas. Mice were anesthetized by intraperitoneal injection of a cocktail (20 μ L/g body weight) containing ketamine (6 mg/mL) and xylazine (0.44 mg/mL) in 10 mM sodium phosphate, pH 7.2, and 100 mM NaCl. Pupils were dilated with 1% tropicamide. Four pictures acquired in the B-scan mode were used to construct each final averaged SD-OCT image.

ERGs.

All ERG procedures were performed by published methods.³⁹ For single-flash recording, the duration of white-light flash stimuli (from 20 μ s to 1 ms) was adjusted to provide a range of

illumination intensities from -3.7 to $1.6 \log \text{cd}\cdot\text{s}\cdot\text{m}^{-2}$. Three to five recordings were made at sufficient intervals between flash stimuli (from 3 s to 1 min) to allow recovery from any photo bleaching effects.

Histology.

Mouse eyes were fixed for 24 h by rocking in a fixation solution (2 mL/eye) containing 4% paraformaldehyde and 1% glutaraldehyde in PBS. The tissue was processed through a series of ethanol, xylene, and paraffin baths in a Tissue-Tek VIP automatic processor (Sakura, Torrance, CA, United States), and 5 μm sections were cut using a Microm HM355 paraffin microtome (Thermo Fisher Scientific, Waltham, MA, United States) and stained with hematoxylin and eosin (H&E). Images of stained sections were captured with a Leica CTR6000 microscope attached to a CCD camera (Micropublisher 5.0 RTV, Qimaging Surrey BC, Canada).

Pharmacokinetic Distribution of *N*-Retinylamides and Ret-NH₂ Derivatives in the Liver and Eye.

Female and male C57BL/6J mice (4-week-old) were randomly divided into seven groups, six treated groups and one control group. Free Ret-NH₂ (3.5 μmol per mouse, dissolved in DMSO and dispersed in vegetable oil) or Ret-NH₂ derivatives (Ret-Gly, Ret-L-Val-Gly, Ret-L-Phe, Ret-L-Leu, or Ret-L-Val, each dissolved in DMSO and dispersed in vegetable oil at 3.5 μmol per mouse) were administered by gastric gavage. The control group was gavaged with drug-free vegetable oil. Then 3 mice were euthanized at each predetermined time point, 2 and 16 h after drug administration. The liver and eye balls were collected to determine tissue *N*-retinylamide content for pharmacokinetic analyses. A portion of the liver tissue (0.3–0.5 g) was weighed and homogenized in 2 mL of a 1:1 ethanol:PBS solution, and the eye balls were similarly processed (eye balls were combined from 3 mice). *N*-Retinylamides were extracted in 4 mL of hexane, concentrated, and reconstituted to a 300 μL volume for liver and 200 μL for eye. Normal-phase HPLC (Agilent-Zorbax SIL; 5 μm ; 4.5 \times 250 mm; flow rate of 1.4 mL/min; 80:20 hexane:ethyl acetate (v:v); detection at 325 nm) was used to determine *N*-retinylamide concentrations in these tissues using a standard curve method.

In Vivo RPE65 Inhibition.

The Ret-NH₂ derivatives (**RVG** and **RF**) or Ret-NH₂ were administered by oral gavage at the same dose of 1.75 μmol per mouse into dark-adapted C57BL/6J wild-type mice (female and male, randomly assigned, $n = 3$) at 16 h prior to the light illumination. After light exposure (7000 lx, 10 min), mice were kept in the dark room for 24 h to allow visual cycle recovery. Mice were then euthanized and eyes were extracted for analyses. Mice without treatment prior to photobleaching were used as controls. Retinoid extraction was done by manually homogenizing eyes in 1 mL of 1:1 ethanol:PBS solution containing 40 mM hydroxylamine. Retinoids were extracted with 4 mL of hexane, concentrated, and reconstituted to a volume of 200 μL . Normal-phase HPLC (Agilent Zorbax SIL; 5 μm ; 4.5 \times 250 mm; flow rate of 1.4 mL/min; 90:10 hexane:ethyl acetate (v:v); detection at 325 nm) was employed to separate retinoids prior to determining their concentrations by comparison

of their absorption spectra with those of synthetic standards. *In vivo* RPE65 inhibition was analyzed by quantifying the amount of 11-*cis*-retinal within each eye.

RPE Microsomal Preparations.

Bovine RPE microsomes, isolated from RPE homogenates by differential centrifugation as previously described,¹⁴ were resuspended in 10 mM Tris HCl, pH 7.2, 1 μ M leupeptin, and 1 mM DTT to achieve a total protein concentration of ~5 mg/mL. To destroy endogenous retinoids, 200 μ L aliquots of RPE microsomes were placed in a quartz cuvette and irradiated for 5 min at 0 °C with a ChromatoUVE transilluminator (model TM-15; UVP).

Retinoid Cycle Enzyme Assays.

All assays were performed under dim red light. A 2 μ L portion of Ret-NH₂ derivative (**RF** or **RVG**) (0.5–10 mM, in DMF) was added into 200 μ L of 10 mM Bis-Tris propane buffer (pH 7.4) containing 150 μ g of RPE microsomes, 1% BSA, 1 mM disodium pyrophosphate, and 20 μ M aporetinaldehyde-binding protein 1 (CRALBP). The resulting mixture was preincubated at room temperature for 5 min. Then 1 μ L of all-*trans*-retinol (20 mM, in DMF) was added and the new mixture was incubated at 37 °C for 1 h. This reaction was quenched by addition of 300 μ L of methanol, and the products were extracted with 300 μ L of hexanes. Production of 11-*cis*-retinol was quantified by normal phase HPLC with 10% (v/v) ethyl acetate in hexanes as the eluent at a flow rate of 1.4 mL/min. Retinoids were detected by monitoring their absorbance at 325 nm and quantified based on a standard curve reflecting the relationship between the amount of 11-*cis*-retinol and area under the corresponding chromatography peak. RPE microsomes without a drug (**RF** or **RVG**) served as 100% controls.

NIH3T3 cells in Dulbecco's Modified Eagle Medium (DMEM) were introduced into 6-well plates and allowed to grow to 90% confluence. Cells then were incubated in DMEM containing 10 μ M all-*trans*-retinol and 4.5 μ M Ret-NH₂ or Ret-NH₂ derivatives for 16 h in the dark. All-*trans*-retinol was included as a positive control and "medium only" served as a negative "no treatment" control. Cells and medium were collected after 16 h of incubation. Samples were treated with 2 mL of methanol, homogenized, and saponified with 1M KOH at 37 °C for 2 h prior to extraction with hexane. The hexane phase was collected, dried in a SpeedVac, and redissolved in 250 μ L of hexane, and retinoid composition was determined by retinoid absorbance after separation by normal phase HPLC.

atRAL Schiff Base Formation.

Incubation of Ret-NH₂ or Ret-NH₂ derivatives **RVG** or **RF** (0.2 mM) with atRAL (2 mM) in ethanol was carried out for 2 h at room temperature. Retinyl imines, separated by reverse phase HPLC, were identified on the basis of both their characteristic UV-vis spectra upon protonation and analysis by mass spectrometry (MS). HPLC conditions were the following: analytical C18 reverse column, 5 μ m, 250 mm \times 4.6 mm, flow rate of 0.5 mL/min, mobile phase acetonitrile:H₂O (v:v) with 0.05% trifluoroacetic acid (0–15 min, acetonitrile from 50% to 100%; 15–30 min, 100% acetonitrile), and detection at 325 nm.

Caco-2 Cell Assay.

Rat tail collagen was diluted 1:9 with 0.5% acetic acid, and the resulting solution (200 μL) was added to each insert to coat the surface. The inserts were air-dried overnight, followed by UV irradiation for 45 min for sterilization. A concentration of 4×10^5 cells/well in DMEM solution containing 20% FBS was added to the precoated insert, and another 2 mL of fresh DMEM medium was added to the opposite bottom side. The medium was changed after the first day of incubation and every other day after that. Cells were cultured for 21 days until they were mature. After aspiration of the medium, cell monolayers were washed with PBS three times. Cells then were incubated with PBS for 1 h at 37 °C to allow release of materials taken up during incubation. After removal of the PBS solution, a drug solution (500 μM in 2.0 mL PBS, pH 6) was loaded onto the apical side and the bottom side was loaded with 2.5 mL of fresh PBS solution. The plates then were incubated at 37 °C, and samples of 200 μL were withdrawn from the bottom side at several time points within 24 h. Amounts of the drug were determined by UV spectrophotometry. Percentage of drug transport was calculated by dividing the amount of drug from the bottom by the total amount of drug added.

ARPE19 Cell Uptake.

ARPE19 cells (human RPE cells purchased from American Type Culture Collection) were plated in 6-well plates using DMEM and allowed to grow to 90% confluence. The cells then were incubated with DMEM containing 10 μM Ret-NH₂ derivatives for 16 h under dark room conditions; cells without drug served as controls. Medium then was removed and cells were washed three times with PBS after incubation for 16 h. Collected cell samples were treated with 400 μL of methanol, homogenized at 37 °C for 1 h, followed by another centrifugation. The supernatant (100 μL) then was subjected to reverse phase HPLC (analytical C18 reverse column; 5 μm ; 250 mm \times 4.6 mm; flow rate of 1.0 mL/min; 60:40 acetonitrile:H₂O (v: v) with 0.05% trifluoroacetic acid; detection at 325 nm) to separate and subsequently determine Ret-NH₂ or its derivatives in serum, as noted above.

Statistical Analyses.

For analyses of the effects of Ret-NH₂ derivatives on light-induced retinal degeneration (Figure 2), each group included at least 5 mice and the thickness of ONL was measured in 4 different areas of the retina for each mouse. To compare the thickness of ONL between Ret-NH₂ derivatives and Ret-NH₂ itself, we used a linear mixed-effects model⁴⁰⁻⁴² with unstructured covariance fitted with SAS Proc Mixed software. All other statistical analyses were performed to compare the treatment groups using one-way ANOVA.

Supplementary Material

Refer to Web version on PubMed Central for supplementary material.

ACKNOWLEDGMENTS

This work was supported in part by funding from the National Eye Institute of the National Institutes of Health (Grant R24EY0211260 and R01EY023948). Further support was obtained through grants from the NIH (NEI R24-EY-024864 and NEI R24-EY-027283) and unrestricted grants from Research to Prevent Blindness to the

Departments of Ophthalmology at UCI. G.Y. was supported by a grant from Knights Templar Eye Foundation (SPN00428). K.P. is the Irving H. Leopold Chair of Ophthalmology. Z.-R.L. is an M. Frank Rudy and Margaret Domiter Rudy Professor of Biomedical Engineering.

REFERENCES

- (1). Evans JB, and Syed BA (2013) New hope for dry AMD? *Nat. Rev. Drug Discovery* 12, 501–502. [PubMed: 23812264]
- (2). Kiser PD, Golczak M, and Palczewski K (2014) Chemistry of the retinoid (visual) cycle. *Chem. Rev* 114, 194–232. [PubMed: 23905688]
- (3). Wolf G (2004) The visual cycle of the cone photoreceptors of the retina. *Nutr. Rev* 62, 283–286. [PubMed: 15384919]
- (4). Berchuck JE, Yang P, Toimil BA, Ma Z, Baciu P, and Jaffe GJ (2013) All-trans-retinal sensitizes human RPE cells to alternative complement pathway-induced cell death. *Invest. Ophthalmol. Visual Sci* 54, 2669–2677. [PubMed: 23518773]
- (5). Murdaugh LS, Avalle LB, Mandal S, Dill AE, Dillon J, Simon JD, and Gaillard ER (2010) Compositional studies of human RPE lipofuscin. *J. Mass Spectrom.* 45, 1139–1147. [PubMed: 20860013]
- (6). Sparrow JR, Fishkin N, Zhou J, Cai B, Jang YP, Krane S, Itagaki Y, and Nakanishi K (2003) A2E, a byproduct of the visual cycle. *Vision Res.* 43, 2983–2990. [PubMed: 14611934]
- (7). Sparrow JR, Wu Y, Kim CY, and Zhou J (2010) Phospholipid meets all-trans-retinal: the making of RPE bisretinoids. *J. Lipid Res.* 51, 247–261. [PubMed: 19666736]
- (8). Mata NL, Weng J, and Travis GH (2000) Biosynthesis of a major lipofuscin fluorophore in mice and humans with ABCR-mediated retinal and macular degeneration. *Proc. Natl. Acad. Sci. U. S. A* 97, 7154–7159. [PubMed: 10852960]
- (9). Murdaugh LS, Wang Z, Del Priore LV, Dillon J, and Gaillard ER (2010) Age-related accumulation of 3-nitrotyrosine and nitro-A2E in human Bruch's membrane. *Exp. Eye Res* 90, 564–571. [PubMed: 20153746]
- (10). Maeda A, Golczak M, Chen Y, Okano K, Kohno H, Shiose S, Ishikawa K, Harte W, Palczewska G, Maeda T, and Palczewski K (2012) Primary amines protect against retinal degeneration in mouse models of retinopathies. *Nat. Chem. Biol* 8, 170–178.
- (11). Kubota R, Boman NL, David R, Mallikaarjun S, Patil S, and Birch D (2012) Safety and effect on rod function of ACU-4429, a novel small-molecule visual cycle modulator. *Retina* 32, 183–188. [PubMed: 21519291]
- (12). Kubota R, Al-Fayoumi S, Mallikaarjun S, Patil S, Bavik C, and Chandler JW (2014) Phase 1, dose-ranging study of emixustat hydrochloride (ACU-4429), a novel visual cycle modulator, in healthy volunteers. *Retina* 34, 603–609. [PubMed: 24056528]
- (13). Dobri N, Qin Q, Kong J, Yamamoto K, Liu Z, Moiseyev G, Ma JX, Allikmets R, Sparrow JR, and Petrukhin K (2013) A1120, a nonretinoid RBP4 antagonist, inhibits formation of cytotoxic bisretinoids in the animal model of enhanced retinal lipofuscinogenesis. *Invest. Ophthalmol. Visual Sci* 54, 85–95. [PubMed: 23211825]
- (14). Golczak M, Kuksa V, Maeda T, Moise AR, and Palczewski K (2005) Positively charged retinoids are potent and selective inhibitors of the trans-cis isomerization in the retinoid (visual) cycle. *Proc. Natl. Acad. Sci. U. S. A* 102, 8162–8167. [PubMed: 15917330]
- (15). Maeda A, Maeda T, Golczak M, Imanishi Y, Leahy P, Kubota R, and Palczewski K (2006) Effects of potent inhibitors of the retinoid cycle on visual function and photoreceptor protection from light damage in mice. *Mol. Pharmacol* 70, 1220–1229. [PubMed: 16837623]
- (16). Yeong JL, Loveman E, Colquitt JL, Royle P, Waugh N, and Lois N (2020) Visual cycle modulators versus placebo or observation for the prevention and treatment of geographic atrophy due to age-related macular degeneration. *Cochrane Database Syst. Rev* 12, CD013154. [PubMed: 33331670]
- (17). Yu G, Wu X, Ayat N, Maeda A, Gao SQ, Golczak M, Palczewski K, and Lu ZR (2014) Multifunctional PEG retinylamine conjugate provides prolonged protection against retinal degeneration in mice. *Biomacromolecules* 15, 4570–4578. [PubMed: 25390360]

- (18). Gynther M, Laine K, Ropponen J, Leppanen J, Mannila A, Nevalainen T, Savolainen J, Jarvinen T, and Rautio J (2008) Large neutral amino acid transporter enables brain drug delivery via prodrugs. *J. Med. Chem* 51, 932–936. [PubMed: 18217702]
- (19). Janoria KG, Boddu SH, Natesan S, and Mitra AK (2010) Vitreal pharmacokinetics of peptide-transporter-targeted prodrugs of ganciclovir in conscious animals. *J. Ocul. Pharmacol. Ther* 26, 265–271. [PubMed: 20565313]
- (20). Eriksson AH, Varma MV, Perkins EJ, and Zimmerman CL (2010) The intestinal absorption of a prodrug of the mGlu2/3 receptor agonist LY354740 is mediated by PEPT1: in situ rat intestinal perfusion studies. *J. Pharm. Sci* 99, 1574–1581. [PubMed: 19780137]
- (21). Rautio J, Kumpulainen H, Heimbach T, Oliyai R, Oh D, Jarvinen T, and Savolainen J (2008) Prodrugs: design and clinical applications. *Nat. Rev. Drug Discovery* 7, 255–270. [PubMed: 18219308]
- (22). Balimane PV, Tamai I, Guo A, Nakanishi T, Kitada H, Leibach FH, Tsuji A, and Sinko PJ (1998) Direct evidence for peptide transporter (PepT1)-mediated uptake of a nonpeptide prodrug, valacyclovir. *Biochem. Biophys. Res. Commun* 250, 246–251. [PubMed: 9753615]
- (23). de Vruhe RL, Smith PL, and Lee CP (1998) Transport of L-valine-acyclovir via the oligopeptide transporter in the human intestinal cell line, Caco-2. *J. Pharmacol Exp Ther* 286, 1166–1170. [PubMed: 9732374]
- (24). Guo A, Hu P, Balimane PV, Leibach FH, and Sinko PJ (1999) Interactions of a nonpeptidic drug, valacyclovir, with the human intestinal peptide transporter (hPEPT1) expressed in a mammalian cell line. *J. Pharmacol Exp Ther* 289, 448–454. [PubMed: 10087037]
- (25). Cocohoba JM, and McNicholl IR (2002) Valganciclovir: an advance in cytomegalovirus therapeutics. *Ann. Pharmacother* 36, 1075–1079. [PubMed: 12022911]
- (26). Reusser P (2001) Oral valganciclovir: a new option for treatment of cytomegalovirus infection and disease in immunocompromised hosts. *Expert Opin. Invest. Drugs* 10, 1745–1753.
- (27). Tsuda M, Terada T, Irie M, Katsura T, Niida A, Tomita K, Fujii N, and Inui K (2006) Transport characteristics of a novel peptide transporter 1 substrate, antihypotensive drug midodrine, and its amino acid derivatives. *J. Pharmacol. Exp. Ther* 318, 455–460. [PubMed: 16597710]
- (28). Katragadda S, Jain R, Kwatra D, Hariharan S, and Mitra AK (2008) Pharmacokinetics of amino acid ester prodrugs of acyclovir after oral administration: interaction with the transporters on Caco-2 cells. *Int. J. Pharm* 362, 93–101. [PubMed: 18638532]
- (29). Golczak M, Imanishi Y, Kuksa V, Maeda T, Kubota R, and Palczewski K (2005) Lecithin:retinol acyltransferase is responsible for amidation of retinylamine, a potent inhibitor of the retinoid cycle. *J. Biol. Chem* 280, 42263–42273. [PubMed: 16216874]
- (30). Sambuy Y, De Angelis I, Ranaldi G, Scarino ML, Stammati A, and Zucco F (2005) The Caco-2 cell line as a model of the intestinal barrier: influence of cell and culture-related factors on Caco-2 cell functional characteristics. *Cell Biol. Toxicol* 21, 1–26. [PubMed: 15868485]
- (31). Zhang J, Dong Z, Mundla SR, Hu XE, Seibel W, Papoian R, Palczewski K, and Golczak M (2015) Expansion of First-in-Class Drug Candidates That Sequester Toxic All-Trans-Retinal and Prevent Light-Induced Retinal Degeneration. *Mol. Pharmacol* 87, 477–491. [PubMed: 25538117]
- (32). Golczak M, Maeda A, Bereta G, Maeda T, Kiser PD, Hunzelmann S, von Lintig J, Blaner WS, and Palczewski K (2008) Metabolic basis of visual cycle inhibition by retinoid and nonretinoid compounds in the vertebrate retina. *J. Biol. Chem* 283, 9543–9554. [PubMed: 18195010]
- (33). Palczewski K (2010) Retinoids for treatment of retinal diseases. *Trends Pharmacol. Sci* 31, 284–295. [PubMed: 20435355]
- (34). Kiser PD, Zhang J, Badiie M, Li Q, Shi W, Sui X, Golczak M, Tochtrop GP, and Palczewski K (2015) Catalytic mechanism of a retinoid isomerase essential for vertebrate vision. *Nat. Chem. Biol* 11, 409–415. [PubMed: 25894083]
- (35). Kiser PD, and Palczewski K (2016) Retinoids and Retinal Diseases. *Annu. Rev. Vis Sci* 2, 197–234. [PubMed: 27917399]
- (36). Anand B, Nashed Y, and Mitra A (2003) Novel dipeptide prodrugs of acyclovir for ocular herpes infections: Bioreversion, antiviral activity and transport across rabbit cornea. *Curr. Eye Res* 26, 151–163. [PubMed: 12815543]

- (37). Rejmanova P, Kopecek J, Duncan R, and Lloyd JB (1985) Stability in rat plasma and serum of lysosomally degradable oligopeptide sequences in N-(2-hydroxypropyl) methacrylamide copolymers. *Biomaterials* 6, 45–48. [PubMed: 3971018]
- (38). Zhang J, Kiser PD, Badiee M, Palczewska G, Dong Z, Golczak M, Tochtrop GP, and Palczewski K (2015) Molecular pharmacodynamics of emixustat in protection against retinal degeneration. *J. Clin. Invest* 125, 2781–2794. [PubMed: 26075817]
- (39). Maeda A, Maeda T, Imanishi Y, Kuksa V, Alekseev A, Bronson JD, Zhang H, Zhu L, Sun W, Saperstein DA, Rieke F, Baehr W, and Palczewski K (2005) Role of photoreceptor-specific retinol dehydrogenase in the retinoid cycle in vivo. *J. Biol. Chem* 280, 18822–18832. [PubMed: 15755727]
- (40). Verbeke G, and Molenberghs G (1997) *Linear mixed models in practice: a SAS-oriented approach*, Springer, New York.
- (41). Laird NM, and Ware JH (1982) *Random-Effects Models for Longitudinal Data*. *Biometrics* 38, 963–974. [PubMed: 7168798]
- (42). Diggle P, Liang K-Y, and Zeger SL (1995) *Analysis of longitudinal data*, Repr. 1994, 1995 (with corrections) ed., Clarendon Press, Oxford University Press, Oxford, NY.

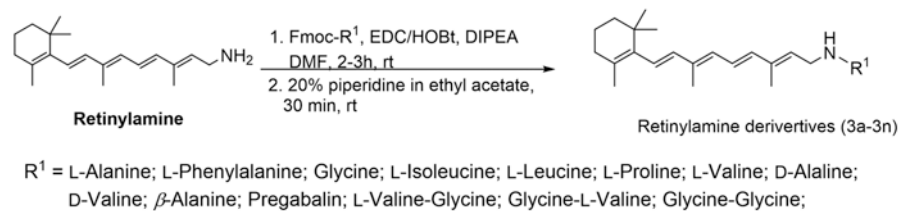


Figure 1.
Synthetic scheme for the retinylamine derivatives.

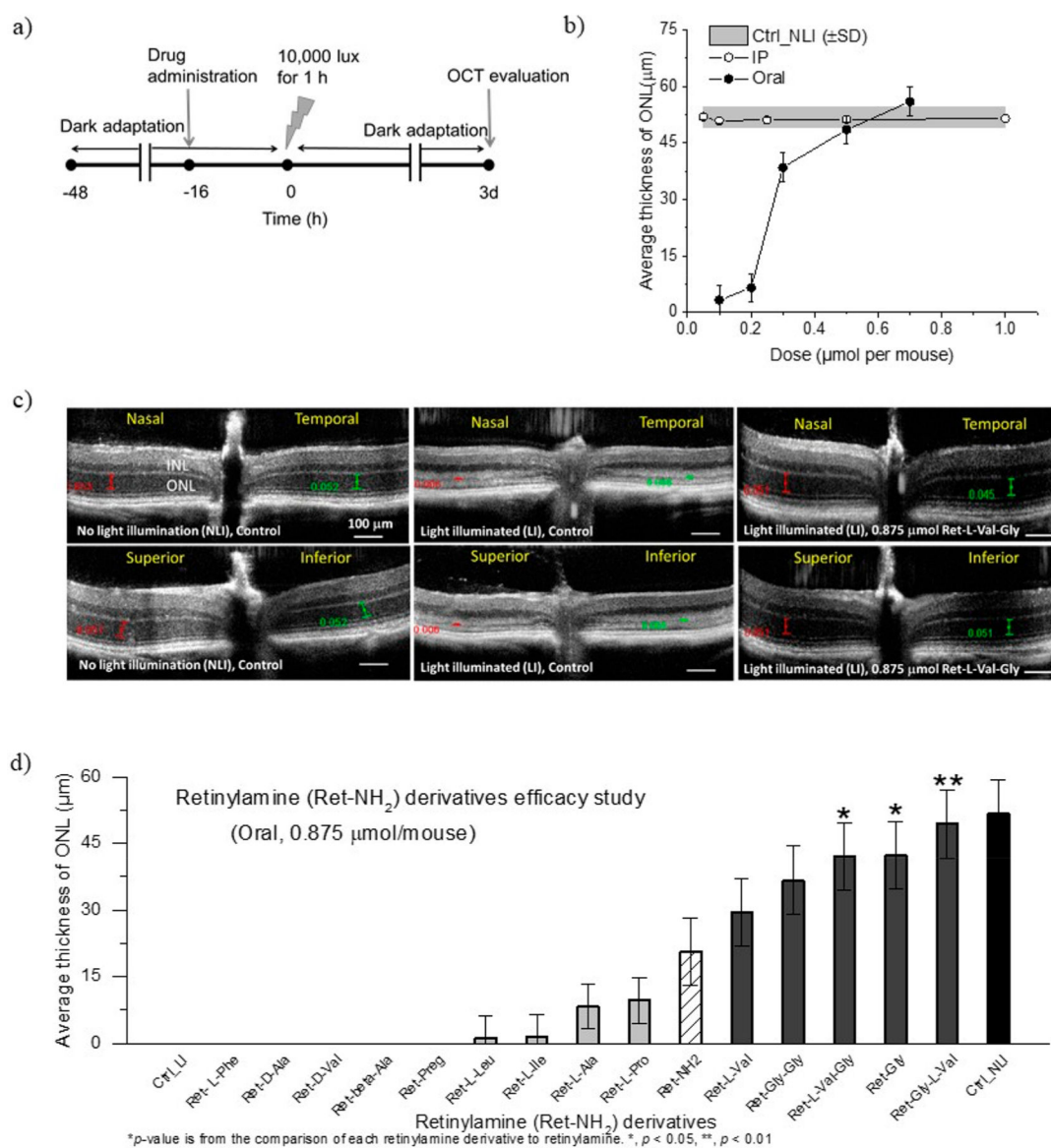


Figure 2. Protective effects of Ret-NH₂ derivatives on the development of acute light-induced retinal degeneration in *Abca4*^{-/-}*Rdh8*^{-/-} mice (NLI = no light illumination; LI = light illuminated). (a) Schematic representation of the experimental design. (b) Ret-NH₂ dose-efficacy curve. (c) OCT images reveal representative morphology of 4-week-old *Abca4*^{-/-}*Rdh8*^{-/-} mouse retinas. Scale bars (red and green) indicate 100 μm in the OCT images. (d) Efficacy study of Ret-NH₂ derivatives *in vivo*. ONL thicknesses (bar heights) represent the average thicknesses measured from OCT images obtained 0.5 mm from the optical nerve at 4 locations (nasal, temporal, superior, and inferior). Five mice were used for each treatment group. Statistical analyses were performed by the linear mixed-effects model with unstructured covariance structure fitted using SAS Proc Mixed software. Error bars indicate SE of the estimated means using a linear mixed-effects model.

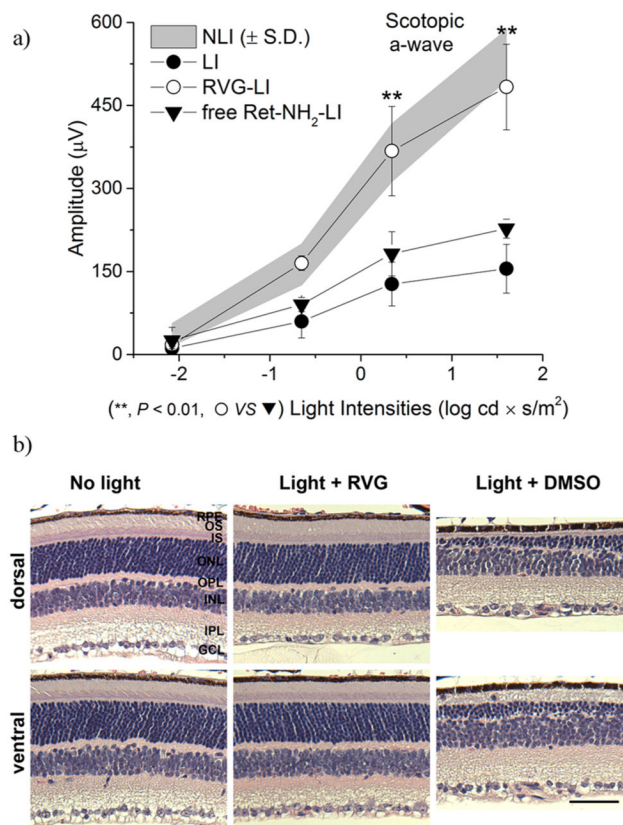


Figure 3.

ERG and histological evaluation for the effectiveness of Ret-L-Val-Gly (**RVG**) on preserving retinal function after light-induced acute retinal degeneration in 4-week-old *Abca4*^{-/-}*Rdh8*^{-/-} mice. (a) Average peak amplitudes of ERG scotopic a-waves for 4-week-old *Abca4*^{-/-}*Rdh8*^{-/-} mice, pretreated with **RVG** or Ret-NH₂ at a dose of 0.875 μmol per mouse 16 h prior to light illumination and evaluation 7 days later (NLI = no light illumination; LI = light illuminated). Error bars indicate SD of the means ($n = 3$). (b) **RVG** protected *Abca4*^{-/-}*Rdh8*^{-/-} mouse retinas from light damage. H&E staining of retinal sections through the dorsal-ventral axis and across the optic nerve head was performed 7 days after light exposure. The histology reveals light-induced retinal degeneration in a vehicle (DMSO)-treated *Abca4*^{-/-}*Rdh8*^{-/-} mice, indicated by a thin outer nuclear layer. Administration of **RVG** before light exposure prevented this retinal damage. RPE, retinal pigment epithelium; OS, outer segment; IS, inner segment; ONL, outer nuclear layer; OPL, outer plexiform layer; INL, inner nuclear layer; IPL, inner plexiform layer; GCL, ganglion cell layer. Scale bar: 50 μm . Statistical analysis was performed to compare the treatment groups using one-way ANOVA.

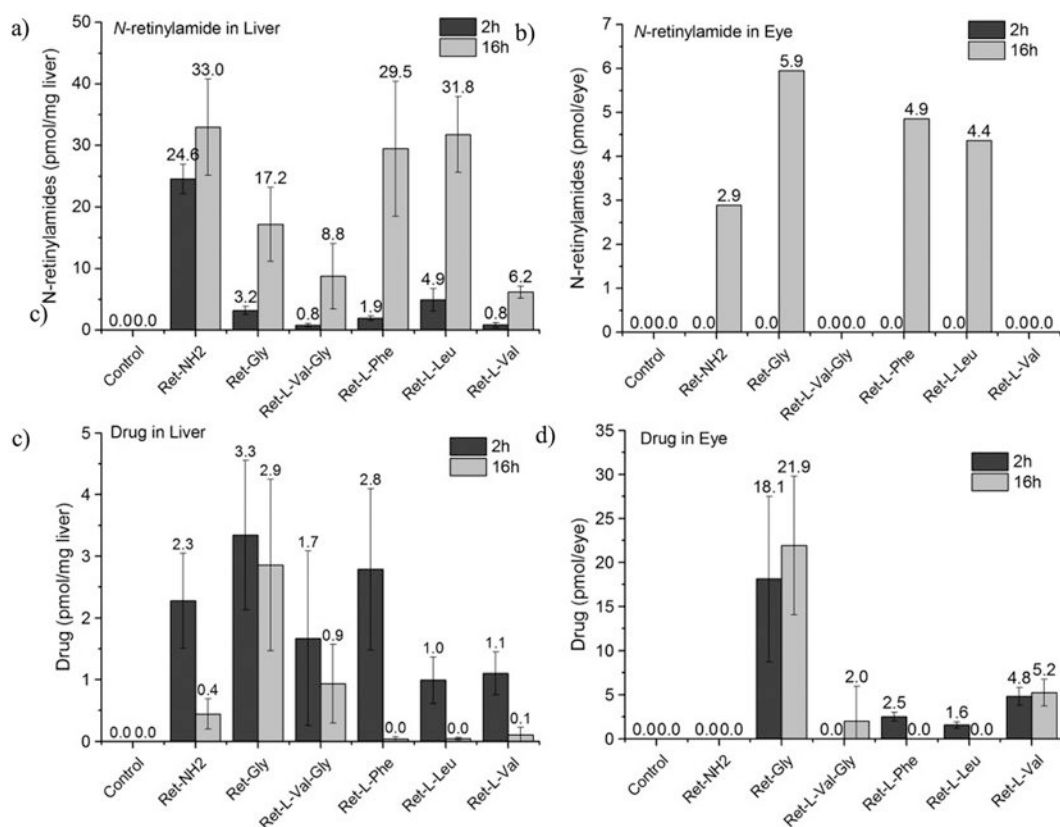


Figure 4.

Biodistribution of *N*-retinylamides from Ret-NH₂ and Ret-NH₂ derivatives (Ret-Gly (RG), Ret-L-Val-Gly (RVG), Ret-L-Phe (RF), Ret-L-Leu (RL), and Ret-L-Val (RV)) in the liver and eye after oral administration. The formulated drugs RG, RVG, RF, RL, RV, or Ret-NH₂ (3.5 μmol per mouse) were orally gavaged into 4-week-old C57BL/6J wild-type mice. Mice then were sacrificed at predetermined time points (2 h or 16 h) after such treatment. *N*-Retinylamides and drugs were extracted from the eyes and liver quantitatively, as determined by HPLC. Error bars indicate SD of the means ($n = 3$).

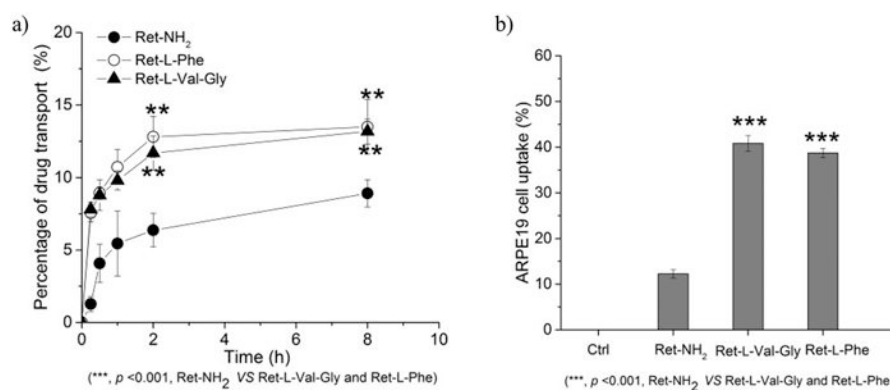
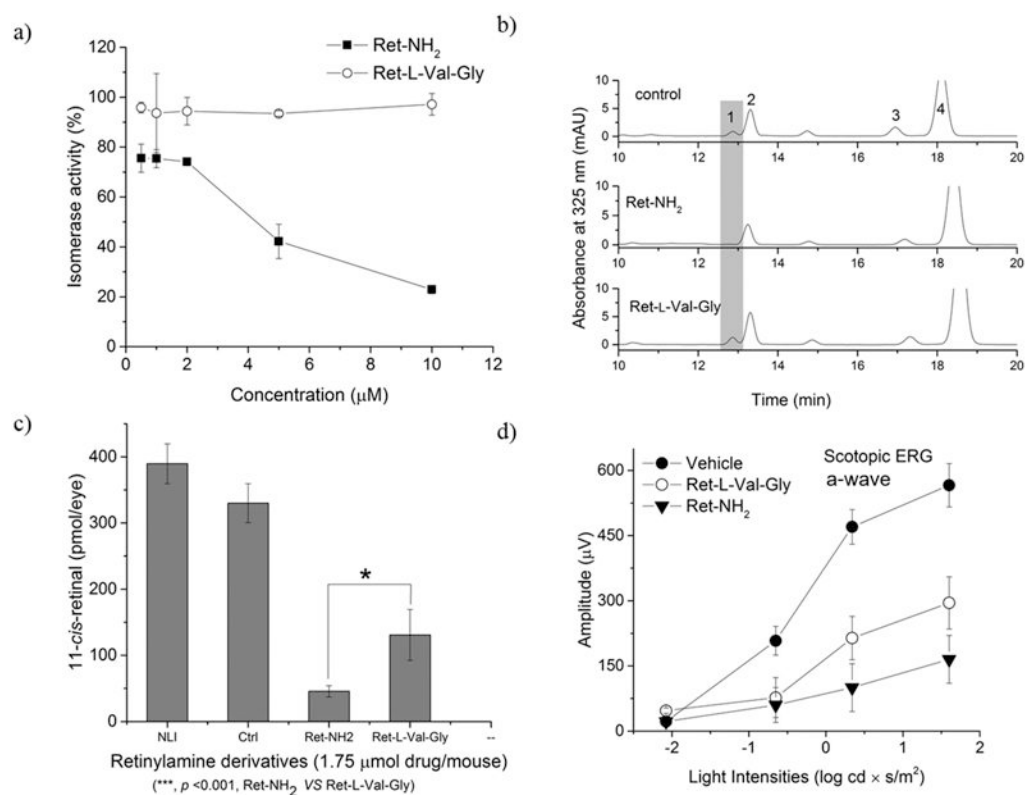


Figure 5. *In vitro* Caco-2 cell transport and ARPE-19 cell uptake assays. (a) Drugs (Ret-NH₂, **RVG**, and **RF**) transport through the Caco-2 cell monolayer. A monolayer of Caco-2 cells was grown on a filter separating two stacked micro well plates into apical (AP) and basolateral (BC) chambers. The permeability of drugs through these cells was determined after their introduction on the AP side of the filter by using UV absorbance to monitor the concentrations of these drugs on the BL side. Percentage of drug transported is calculated by dividing the amount of drug on the BL side by the total amount of drug added on the AP side. (b) Cellular uptake of the drugs by ARPE19 cells. After co-incubation of ARPE19 cells with selected drugs (**RVG**, **RF**) for 16 h, the medium was removed and cells were collected. Drugs were extracted from the cells and analyzed by HPLC. ARPE19 cells without the drug served as controls. Statistical analysis was performed to compare the treatment groups using one-way ANOVA.

**Figure 6.**

Inhibition of 11-*cis*-retinol production by Ret-NH₂ or Ret-NH₂ derivatives (RVG). RPE microsomes were incubated for 1 h with each compound at concentrations of 0.5–10 μM in the presence of 10 μM all-*trans*-retinol. (a) Dose-dependent effects of inhibitors on 11-*cis*-retinol production by RPE microsomes. RPE microsomes without drug (RF or RVG) served as 100% controls. (b) NIH3T3 cell culture experiment. Cells were incubated with 10 μM all-*trans*-retinol in addition to 4.5 μM of each drug (Ret-NH₂ or RVG) in growth medium for 16 h prior to extraction with organic solvent. Concentrations of 11-*cis*-retinoids were determined by HPLC 16 h after cell homogenization, saponification, and retinoid extraction. Peaks were identified based on their elution times and absorbance spectra that were identical with synthetic standards (1, 11-*cis*-retinol; 2, 13-*cis*-retinol; 3, 9-*cis*-retinol; 4, all-*trans*-retinol; mAU, milli absorbance units). (c) Comparison of 11-*cis*-retinal regeneration in mice treated with selected Ret-NH₂ derivatives. Dark-adapted C57BL/6J mice were given the dose of inhibitor (1.75 μmol/mouse) by oral gavage 16 h before they received a retinal bleach for 10 min at 7000 lx. Regeneration of 11-*cis*-retinal continued for 24 h in the dark, after which ocular retinoids were extracted and separated by normal phase HPLC. (d) Average peak amplitudes of ERG scotopic a-waves for 4-week-old WT mice after treatment with free Ret-NH₂ or RVG. After 4-week-old C57BL/6J WT mice were kept in the dark for 48 h, they were given either Ret-NH₂ or RVG at a dose of 1.75 μmol per mouse by gastric gavage 16 h prior to ERG evaluation. Statistical analysis was performed to compare the treatment groups using one-way ANOVA.

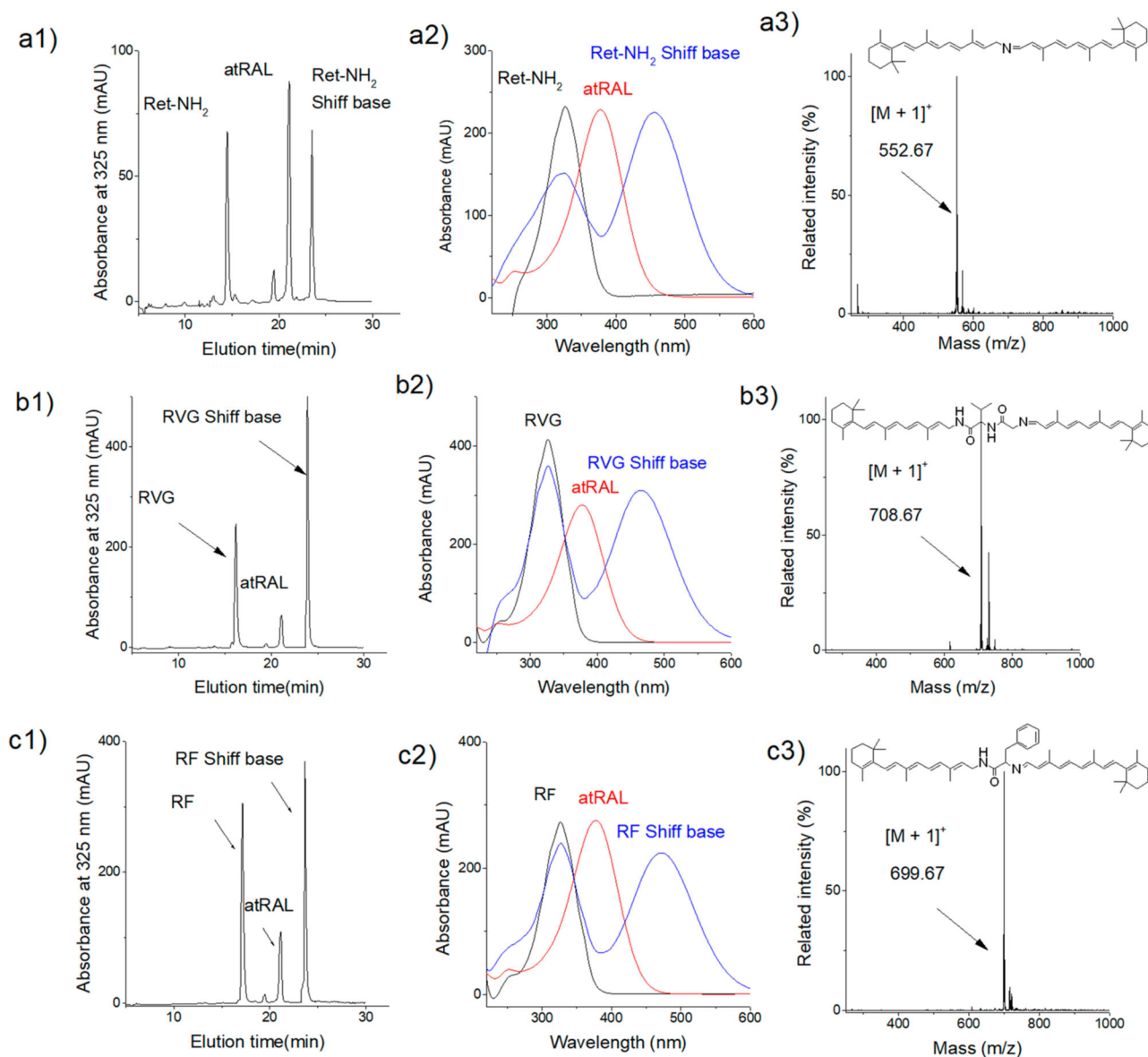


Figure 7. Identification of all-*trans*-retinal Schiff base adducts. Ret-NH₂ derivatives **RVG** and **RF** (0.2 mM) were incubated with all-*trans*-retinal in ethanol for 2 h at room temperature and then analyzed by HPLC and LC-MS. Schiff base adducts were detected at 460 nm. (a1, b1, and c1) HPLC elution profiles after the Schiff base reaction. (a2, b2, and c2) Corresponding UV-vis spectra of reaction materials and the resulting Schiff base adducts. (a3, b3, and c3) Mass spectra of the corresponding protonated Schiff base adducts.

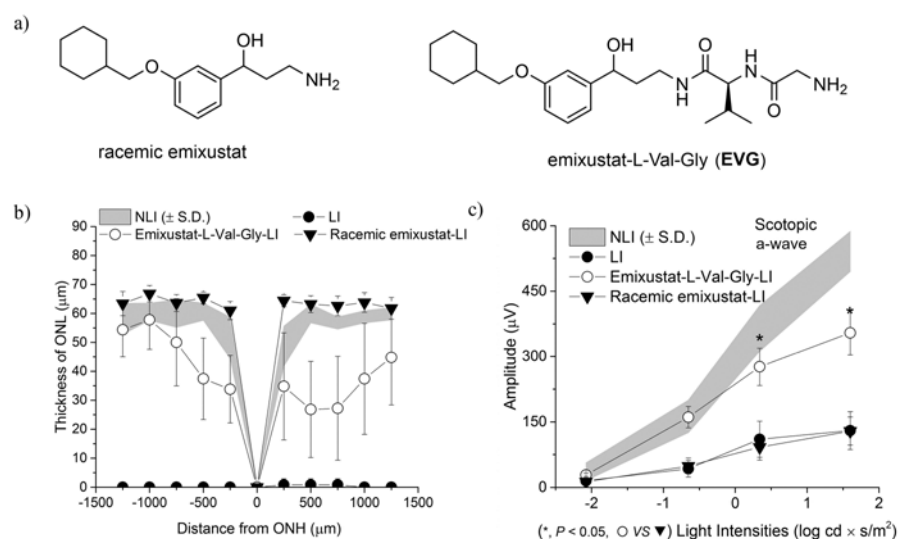
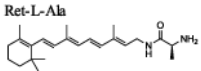
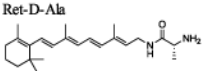
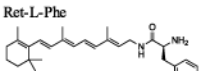
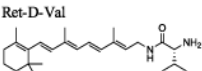
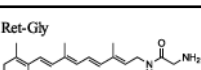
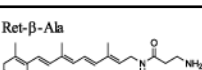
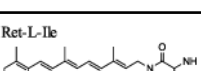

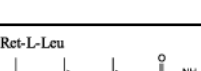
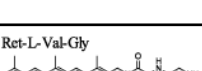
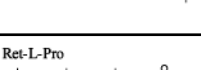
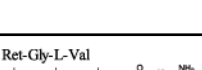
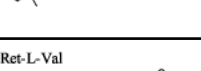
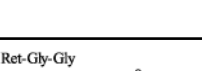


Figure 8.

Protective effects of emixustat-L-Val-Gly (**EVG**) against light-induced acute retinal degeneration in 4-week-old *Abca4^{-/-}Rdh8^{-/-}* mice. (a) Structures of racemic emixustat and emixustat-L-Val-Gly (**EVG**). 4-week-old *Abca4^{-/-}Rdh8^{-/-}* mice were kept in the dark for 48 h, then they were given either emixustat or **EVG** at a dose of 1.90 µmol per mouse by gastric gavage 16 h prior to light illumination; OCT and ERG evaluations were done 7 days later (NLI = no light illumination; LI = light illuminated). (b) ONL thicknesses were measured from *in vivo* OCT images obtained along the vertical meridian from the superior to inferior retina of mice. (c) Average peak amplitudes of ERG scotopic a-waves for 4-week-old *Abca4^{-/-}Rdh8^{-/-}* mice. Statistical analysis was performed to compare the treatment groups using one-way ANOVA. Error bars indicate SD of the means ($n = 5$).

Table 1.Chemical Structure of Amino Acid and Peptide Derivatives of Ret-NH₂

Compound	Abbreviation	Compound	Abbreviation
Ret-L-Ala 	RA	Ret-D-Ala 	RdA
Ret-L-Phe 	RF	Ret-D-Val 	RdV
Ret-Gly 	RG	Ret-β-Ala 	RbA
Ret-L-Ile 	RI	Ret-Preg 	RPreg
Ret-L-Leu 	RL	Ret-L-Val-Gly 	RVG
Ret-L-Pro 	RP	Ret-Gly-L-Val 	RGV
Ret-L-Val 	RV	Ret-Gly-Gly 	RGG